

A Methodological Assessment of Phase-Rectified Signal Averaging through Simulated Beat-to-Beat Interval Time Series

Roberto Sassi¹, Tamara Stampalija², Daniela Casati³, Enrico Ferrazzi³, Axel Bauer⁴, Massimo W. Rivolta¹

¹ Dipartimento di Informatica, Università degli Studi di Milano, Italy

² Institute for Maternal and Child Health, IRCCS Burlo Garofolo, Trieste, Italy

³ Department of Biomedical and Clinical Sciences, Università degli Studi di Milano, Italy

⁴ Medizinische Klinik der Universität München, Munich, Germany

Abstract

Average cardiac acceleration (AC) and deceleration (DC) capacity, as computed by Phase-Rectified Signal Averaging (PRSA), were introduced to detect quasi-periodic oscillations in RR series. Calculation of AC and DC depends on three parameters (T , L and s). The aim of the study was to provide further insights on AC/DC and on the appropriate selection of these parameters.

Numerical simulations were focused on: i) changing the frequency of the oscillations detected by AC/DC; ii) testing the difference between AC and DC on synthetic data generated by AR models, fitted on real RR series; and iii) the effect of different growing and decreasing trends (lack of time-reversal symmetry).

When computed on series generated by AR models, AC and DC were quantitatively equivalent, independently of the power spectrum ($p < 0.05$). The parameter s , more than T , affected the results, while values of $L > s$ were equivalent. In fact, s selected the oscillations to which AC/DC resulted maximally sensitive. On the contrary, sawtooth-like series, with different growth and decrease rates, showed a marked difference between AC and DC.

AC and DC are not simply related to spectral contents. Indeed, AC and DC are linked to the asymmetries between the rates of growth and decrease of heart rate, and might quantify differently underlying regulatory mechanisms.

1. Introduction

Phase-Rectified Signal Averaging (PRSA) is a methodology capable of extracting quasi-periodic oscillations (*i.e.*, many periodic patches, of which the average length defines the *coherence time* of the quasi-periodicity) out of noisy and non-stationary signals [1]. The aim of such technique is to transform the signal into a much shorter sequence, *i.e.*, the PRSA series, in which only the relevant quasi-periodicities of the original series are present.

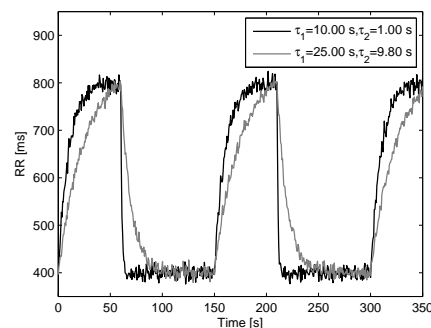


Figure 1. Synthetic sawtooth-like signals (with different time-constants), mimicking changes in RR series typical of umbilical cord occlusion in fetal animal models.

When applied on cardiac beat-to-beat interval time series (RR), PRSA is used to quantify the average cardiac acceleration (AC) and deceleration (DC) capacity of the heart rate. In fact, phase de-synchronizations are common in RR series, due to extrinsic noise (*e.g.*, runs of misdetected beats and signal losses) or due to intrinsic phase-resettings (*e.g.*, ectopic beats). AC and DC have proven to be predictors of risk in several clinical scenarios [2–5]. Of note, Bauer *et al.* [2] showed that DC was a better predictor of risk after myocardial infarction than left-ventricular ejection fraction (LVEF) and standard deviation of normal-to-normal intervals (SDNN).

A complete description of the procedure can be found in [1]. Briefly, anchor points are identified within the series. Each sample $x[t]$ satisfying the condition

$$\frac{1}{T} \sum_{i=0}^{T-1} x[t+i] > \frac{1}{T} \sum_{i=1}^T x[t-i] \quad (1)$$

is included into the deceleration anchor points' list. The acceleration anchor points' list is instead built by changing the direction of the inequality (1). Then, a window of length $2L$ is aligned on each anchor point (from $t-L$

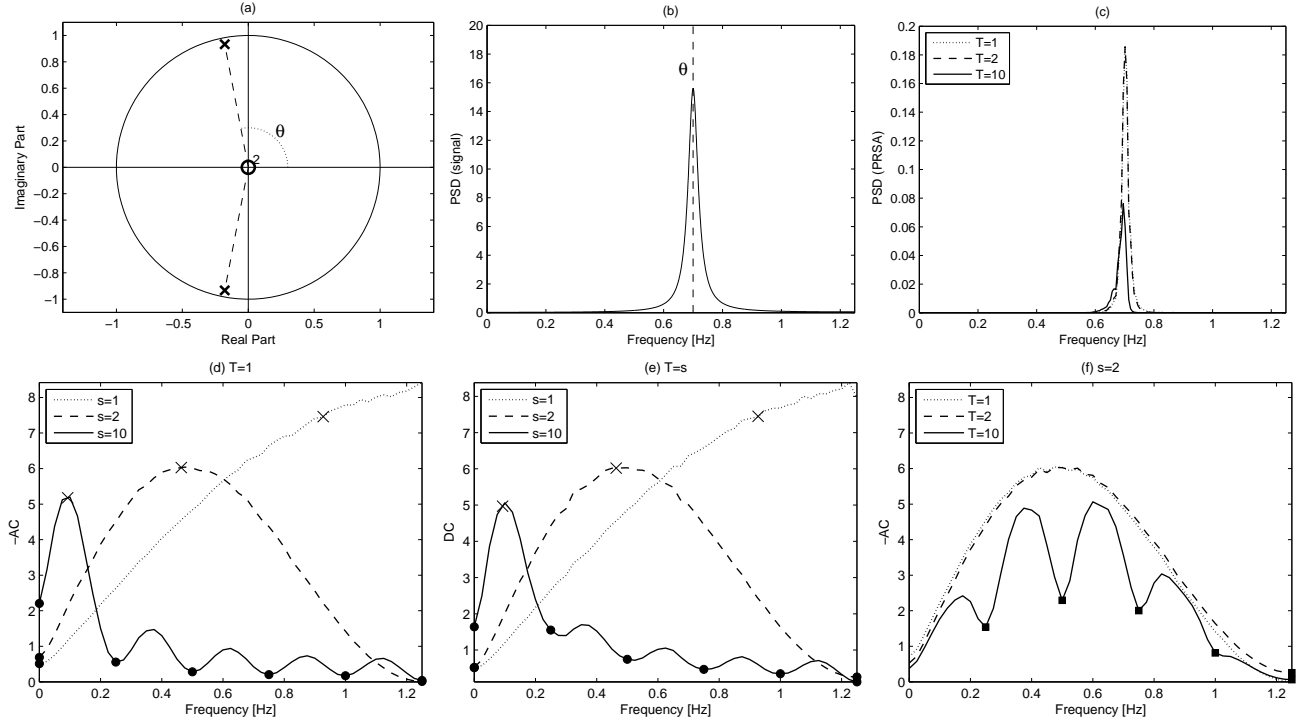


Figure 2. Values of -AC and DC (panels d-f) for various combinations of the parameters T and s , on series generated from the 2nd order AR model $H_{AR}(z) = 1 - 2\rho \cos \theta z^{-1} + \rho^2 z^{-2}$, with $\rho = 0.95$. The poles' phase θ (panel a) was varied, while driving the model with a WGN of variance $\sigma_w^2 = [1 - \rho^6 + (\rho^2 - \rho^4)(1 - 4 \cos^2 \theta)] / (1 + \rho^2)$, such that the signals' power was fixed at $\sigma_y^2 = 1$. The power spectra of the series (panel b) and PRSA signals (panel c) were concentrated around the frequency $f = \theta / (2\pi f_s)$. However, the low-pass FIR filter of order $T - 1$, $H_T(z) = (z^T - 1) / [Tz^{T-1}(z - 1)]$, applied in eq. (1) before the selection of the anchors points, reduced the PRSA's amplitude for frequencies close to its zeros. While not acting directly on the PRSA, the filter reduces the likelihood that related samples will turn into anchor points. In panel (d) and (e), the sign \times marks the frequency to which AC/DC should be more sensitive, as predicted theoretically by $0.371 f_s / s$ Hz (please note that in [1] the formula was derived for $s = T$). Also, a \bullet sign locates the zeros of the high-pass FIR filter of order $2s - 1$, $H_s(z) = (z^s - 1)^2 / [2sz^s(z - 1)]$, imposed on PRSA by the Haar wavelet transform of eq. (2). Finally, the symbol \blacksquare , in panel (f), indicates the zeros of the low-pass filter $H_T(z)$

to $t + L - 1$). The segments of signal x , located by each window, are finally averaged obtaining the PRSA series. Hence the PRSA calculation depends on two parameters: T affects the selection of the anchor points and L defines the length of the PRSA series. A wavelet transform (using a Haar mother wavelet function) of the PRSA series, evaluated at scale s (a third free parameter) and location $L + 1$, is employed to derive the capacities:

$$\text{DC (or AC)} = \sum_{i=1}^s \frac{\text{PRSA}(L+i)}{2s} - \sum_{i=0}^{s-1} \frac{\text{PRSA}(L-i)}{2s}. \quad (2)$$

Despite the proven capability of AC/DC on several clinical scenarios, what they can really capture on RR series, and what roles the parameters play, are still matter of investigation. For example, it is unclear to what extent AC and DC are correlated with the autonomic nervous system (ANS) modulations. Furthermore, the values of the param-

eters on which AC/DC are dependent have been typically set to those that provided the best classification rate for the specific application (e.g., $T = 1$ and $s = 2$ in [2]).

We performed an extensive set of numerical simulations in order to provide insights about the meaning of AC/DC and on the effects of the parameters. In particular, the aims of the study were to: i) further clarify the influence of the parameters T and s on AC/DC; ii) evaluate the inter-correlation between AC and DC on synthetic series.

2. Methods

Three different sets of numerical simulations were prepared. $L = 40$ was consistently employed in all of them.

First, the changes induced on AC/DC by different power spectra were evaluated varying the phase of the poles of a 2nd order autoregressive (AR) model, between 0 and π

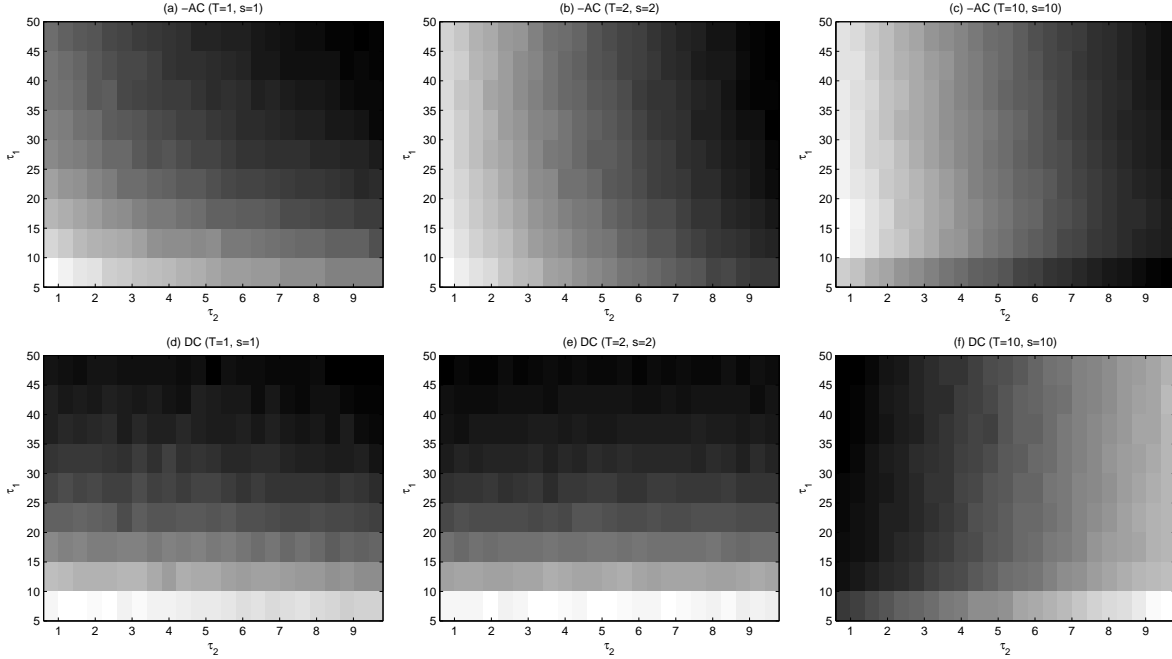


Figure 3. Values of -AC and DC for sawtooth-like signals for $T = s$, when varying the time-constants τ_1 and τ_2 . For display purposes, values were rescaled in the interval 0 (black) to 1 (white).

(step 0.01), while normalizing the variance of the signals at 1 (the PRSA signal depends linearly on the variance of the series). Average measures were determined on 30 realizations of 3000 samples each. The hypothetical heart rate was set to 150 bpm ($f_s = 2.5$ Hz). Such analysis was repeated for s between 1 to 20 and $T = s$ or $T = 1$.

Synthetic signals, obtained from 2nd order AR models, contained only a single periodic component. To have more realistic series (in adult human heart rate at least 3 components are present, typically labelled VLF, LF and HF), 93 AR models were fitted on 300 samples-long artifacts-free RR series, one for each subject in the Physionet's *nrsr2db* (healthy) and *chf2db* (congestive heart failure) databases. Models' orders were significantly larger than 2 (minimum model order was 8, fulfilling Akaike's information criterion and Anderson's whiteness test). For each AR model, average AC and DC values were determined on 30 synthetic series, varying $s = T$ from 1 to 20. The power of the signals was normalized to 1.

Sawtooth-like heart rate trends¹ (e.g., fig. 1) were employed for the third set of simulations, to assess the impact of time-reversal symmetry (or lack-of, as in asymmetric trends, i.e., displaying different time-constants for the growing and decreasing traits) on AC/DC. Trends y were

¹Sawtooth-like RR series are common, for example, in sport medicine, e.g., intervals training, or in fetal animal models, e.g., umbilical cord occlusions (UCO). Within the context of UCO, the term u in equation 3 models the pressure signal occluding the umbilical cord and the series y varies from 400 to 800 ms, which is typical for a sheep fetus.

generated solving the ordinary differential equation:

$$\dot{y} = -\tau_2^{-1}y - (\tau_1^{-1} - \tau_2^{-1})uy + u, \quad (3)$$

where u is the external input ($u = 1$ determines the presence of the trend), and τ_1 and τ_2 are the time-constants of the growing and decreasing traits, respectively. For the simulations, τ_1 was varied from 5 to 50 and τ_2 from 1 to 10. Finally, white Gaussian noise was added to y (signal-to-noise ratio: 25 db). Average values of AC/DC were obtained from 30 realizations, using $s = T$.

3. Results

3.1. Varying location of AR models' poles

First, the mean value of AC (or DC), for a given phase of the poles of the 2nd order AR models, was more affected by s than T (fig. 2d-f). Hence s played a major role on selecting the frequency of the oscillations which most influenced AC/DC. Changing T surely modified the PRSA series by limiting its frequency content. However, if PRSA is subsequently used to assess AC/DC, the band-pass filtering effects imposed by eq. (2) are predominant (fig. 2f) and changing T only affects frequencies in the neighborhoods of the zeros of the low-pass filter applied on both side of eq. (1). Second, no relevant differences were detected between -AC and DC for any values of s and T (fig. 2d and 2e). The latter findings were quantitatively

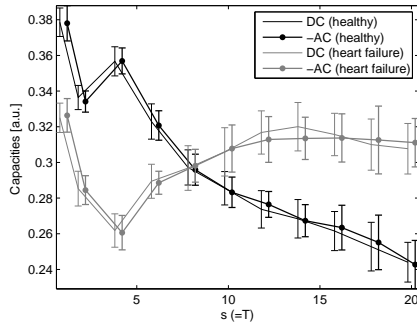


Figure 4. Mean (\pm standard deviation) -AC and DC values for signals generated by two AR models fitted on a healthy and heart failure subjects.

confirmed on higher order models, where the mean values of -AC and DC were not statistically different within the same AR model (t -test, $p < 0.05$). However, AC (and DC) differed between models for a large range of $s = T$ values (see fig. 4 for an example).

3.2. Sawtooth-like heart rate trends

Notwithstanding they resulted practically identical on AR models in section 3.1, -AC and DC clearly differed when using sawtooth-like signals (fig. 3) with asymmetric trends. Indeed, both capacities varied independently, and DC was modulated by τ_1 , which determines the growing trends (the “decelerating” part of the series) and, on the opposite, AC by τ_2 (the time-constant which dictates the “accelerations” in the sequence).

However, when employing small values of T , while DC was largely independent from τ_2 (fig. 3d and 3e), AC was also slightly dependent on τ_1 (fig. 3a and 3b). This is due to the fact that for $\tau_1 \gg T$, simply due to short erratic fluctuations, AC anchor points were selected also on the growing trends. On the other hand, for larger values of T , the number of points in the decaying trends was comparable to T , reducing the number of DC anchor points close to the transitions (and viceversa, increasing the number of AC anchor points). This resulted in an increased dependence of DC on τ_2 (fig. 3f).

4. Conclusion

The value of s , more than T , determines the frequency band (centered around $f = 0.371f_s/s$) of the oscillations which lead to larger AC/DC values, at a fixed signal’s power. On the other hand, the value of T plays a major role in the selection of the anchor points, and it should be smaller than the average time-constant of the trends of interest (e.g., τ_1 and τ_2 in fig. 3).

Moreover, a difference between the values of -AC and

DC does not depend on the shape of the power spectrum, which is unchanged after time-reversal of the series (the anchor points of AC become those of DC). In fact, -AC and DC did not differ in AR models with largely different spectral content. A difference between the two capacities was found only when asymmetries in time-constants of growing and decaying trends were present. Hence, AC and DC do not simply reflect the change in power of selected frequency bands contained in the series. On the contrary, they are strictly related to asymmetries present in the time series, and so they might quantify different underlying regulatory mechanisms, as in [2] where the predictive value of DC was higher than that of AC.

Of minor relevance, the simulations also confirmed that L should be larger than the length of the period of the slowest oscillation of interest, and AC/DC are linearly dependent on the power of the signal.

A limitation of the study was that we only employed simulated series to study the effects of T and s on AC/DC. A large study on the predictive value of DC in post-MI patients [2], obtained optimal results for $s = T + 1$. Therefore, from a clinical point of view, it is not clear if the selection of s and T should be separated, and preliminary tests might be of help in each specific application.

References

- [1] Bauer A, Kantelhardt JW, Bunde A, Barthel P, Schneider R, Malik M, Schmidt G. Phase-rectified signal averaging detects quasi-periodicities in non-stationary data. *J Phys A* 2006;364:423–434.
- [2] Bauer A, Kantelhardt JW, Barthel P, Schneider R, Mäkikallio T, Ulm K, Hnatkova K, Schömig A, Huikuri H, Bunde A, Malik M, Schmidt G. Deceleration capacity of heart rate as a predictor of mortality after myocardial infarction: cohort study. *Lancet* 2006;367:1674–1681.
- [3] Kantelhardt JW, Bauer A, Schumann AY, Barthel P, Schneider R, Malik M, Schmidt G. Phase-rectified signal averaging for the detection of quasi-periodicities and the prediction of cardiovascular risk. *Chaos* 2007;17:015112.
- [4] Huhn EA, Lobmaier S, Fischer T, Schneider R, Bauer A, Schneider KT, Schmidt G. New computerized fetal heart rate analysis for surveillance of intrauterine growth restriction. *Prenat Diagn* 2011;31:509–514.
- [5] Rivolta MW, Stampalija T, Casati D, Richardson BS, Ross MG, Frasc MG, Bauer A, Ferrazzi E, Sassi R. Acceleration and deceleration capacity of fetal heart rate in an *in-vivo* sheep model. *PLoS ONE* 2014;9:e104193.

Address for correspondence:

Roberto Sassi

Dipartimento di Informatica, Università degli Studi di Milano
via Bramante 65, 26013 Crema (CR) Italy

E-mail: roberto.sassi@unimi.it